The Development of Chorus, Source, and Seed Electrons, and the Radiation Belt Response During CME and CIR Storms

S. Bingham[1], C. G. Mouikis[1], L. M. Kistler[1], A. J. Boyd[2], K. Paulson[1], C. Farrugia[1], C. L. Huang[1], H. E. Spence[1], S. G. Claudepierre[3], C. Kletzing[4]

[1]SSC, Eos, Univ. of New Hampshire, Durham, USA, [2]New Mexico Consortium, Los Alamos, New Mexico, USA, [3]Space Sciences Department, The Aerospace Corporation, El Segundo, California, USA, [4]Department of Physics and Astronomy, University of Iowa, Iowa City, Iowa, USA.

Introduction

- Gyroresonant wave-particle interactions between chorus and 100s of keV seed electrons can lead to radiation belt enhancements.
- Temperature anisotropy of 10s of keV source electrons 10s of keV provides the free energy for chorus waves.
- Source & seed electron access to the inner magnetosphere is dependent on convection, sub-storm activity, and conditioning in the plasmasheet.
- Differences in the characteristic solar wind of CMEs and CIRs can create differences in the energy spectrum/ composition of the plasmasheet, convection, and substorm activity.

Figure 1

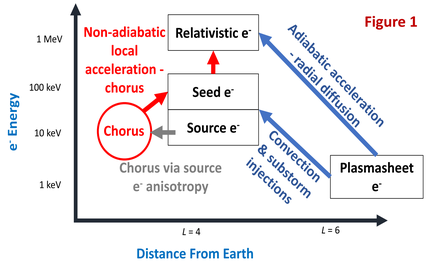

- The **Van Allen Probes** (RBSP) are used to create a **storm phased epoch analysis** of **chorus wave power** and **plasma conditions driving chorus activity** - via a linear theory proxy - **during CME/CIR storms**.
- **RBSP** is also used to create a **superposed epoch analysis** of the growth of the **seed** and **radiation belt** electrons vs L^* **during CME/CIR storms**.

Data and Storm Selection

Van Allen Probes

- **HOPE** – e^- < 60 keV. **MagEIS** – e^- 30 keV to 3 MeV.
- **REPT**– e^- 1–20 MeV. **EMFISIS** – magnetometer and waves instrument.

Storm Selection

- **25 CME** and **35 SIR/CIR Storms** are **identified between 2013-01-01 and 2016-04-16** with a minimum *Dst** between -50 and -150 nT.
- Storm selection **required a single identifiable driver** (CME/CIR). Periods after the start of a second dip in *Dst* were not used.
- Fig 2: **median**, mean, and quartile superposed epoch sw for CMEs/CIRs. Main phase normalized to 12 hrs.

Figure 2 CME — Median Mean Quartiles — CIR

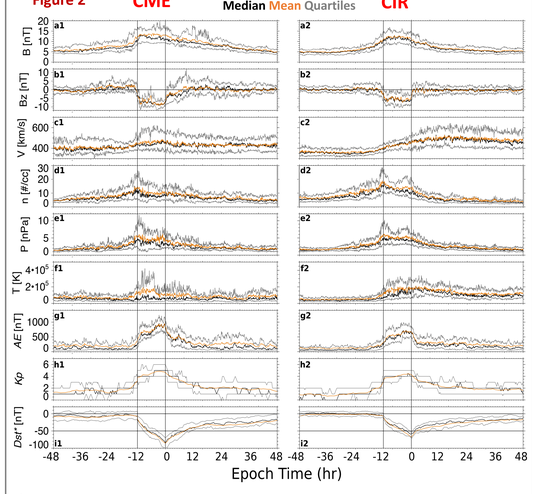

- Fig 3: RBSP *MLT/L* coverage during CMEs/CIRs.
- **CMEs – greater substorm activity** and **stronger convection**.
- **CIRs – higher n_{sw}, v_{sw}, and T_{sw}.**

CME Figure 3 CIR

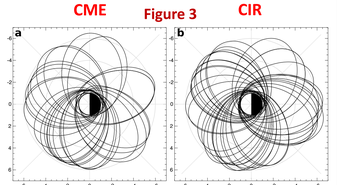

Chorus Wave Activity and Source Electron Development During CMEs and CIRs

- Gary et al. [2005] developed a **linear theory proxy inferring chorus growth from plasma parameters**.
- **Proxy for chorus growth**, Σ_e, is a **product of** the hot (0.03-60 keV) **electron anisotropy**, A_e, and **hot electron** $\beta_{e,\parallel}$:

$$\Sigma_e = \left(\frac{T_{e,\perp}}{T_{e,\parallel}} - 1\right)\beta_{e\parallel}^{\alpha} \qquad \beta_{e,\parallel} = \frac{n_e k T_{e,\parallel}}{B^2/2\mu_0}$$

- RBSP used to measure average CME/CIR chorus power and proxy components: (a) observed chorus wave power, (b) hot e^- pressure, (c) hot e^- n_e, (d) hot e^- $T_{//}$, (e) hot e^- $\beta_{e,\parallel}$, (f) hot electron anisotropy ($A = T_{e\perp}/T_{e\parallel} - 1$), and (g) proxy growth.
- Chorus: integrated wave power between 0.05–0.8 f_{ce} when RBSP outside of plasmasphere with ellipticity > 0.7 & planarity > 0.6
- **Chorus power is comparable between CMEs/CIRs**
- **Strongest chorus** in **main phase** on **dawn/pre-dawn** sector. **Decreases** but **spreads across dayside** in recovery phases.
- **Source electrons** (1-60 keV) **quickly reach dawn** with **enhanced convection** during the **main phase**.
- Asymmetric **source electron ring current forms** a weaker, but **symmetric ring current** during the **recovery phase**.
- **Chorus activity follows the drift paths of source electrons**
- **During recovery phases**, **source electrons drift across the dayside**, however their overall **flux levels drop as open/closed drift boundaries change**.
- **Location of growth proxy**, Σ_e, **correlates well with measured chorus** power.
- Changes to the hot electron pressure and plasma beta are mainly driven by enhancements to the hot electron density.

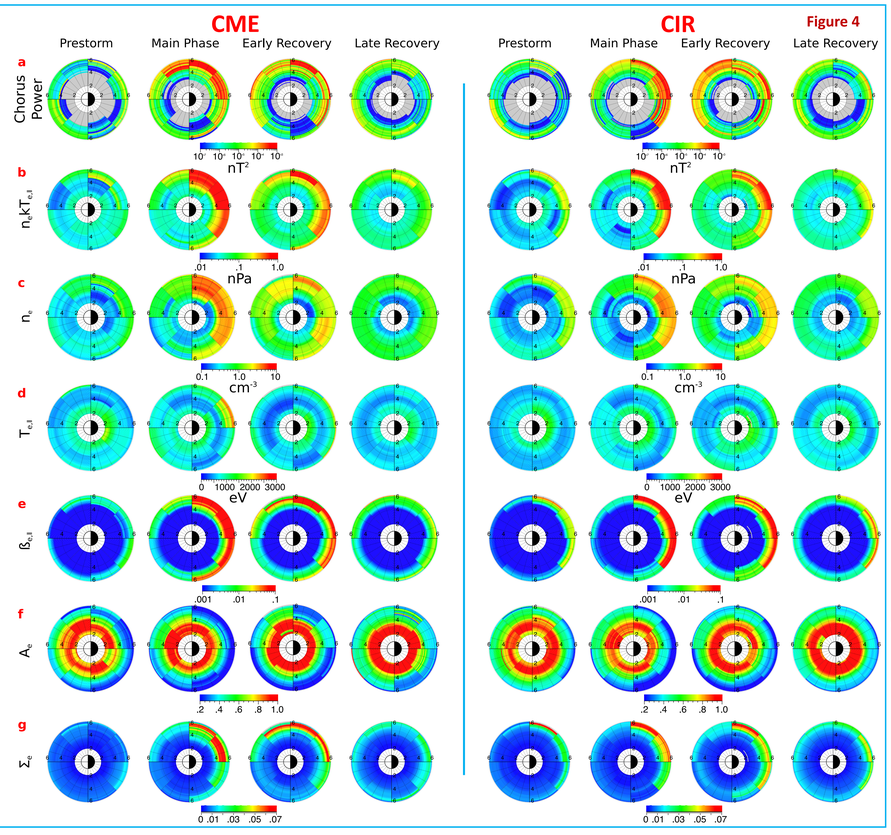

Figure 4

Summary

- **Similar** levels of **chorus activity during CME** and **CIR** driven storms.
- Observe **MLT/storm phase dependence** of **chorus wave power.**
- **Wave power follows changing open/closed drift paths of** 10s of keV **source electrons** during storm times.
- **Stronger, earlier, and deeper** penetrating **seed e^- enhancements during CME storms**.
- **Greater likelihood** of **overlap** between **seed** enhancement and **chorus during CME storms**.
- **Radiation belt enhancement** occurs **more often during CME** storms and reaches **lower L^*.**
- **PSD profile of CME RB enhancement** has **signs of local acceleration**.
- **Larger seed enhancement is** possibly driven by **greater substorm activity** and **convection in CME storms**.

Acknowledgements and References

This work has been supported by the NASA NNX14AC88G grant, NASA Contract Number NNN06AA01C - Phase E Extended Mission 2 (ARDES), and the **NH Space Grant Consortium** under **NASA grant NNX15AH79H**.

Boyd, A. J. et al., (2016), Statistical properties of the radiation belt seed population, JGR SP, doi:10.1002/2016JA022652.

Gary, S. P. et al., (2005), Electron anisotropy constraint in the magnetosheath: Cluster observations, GRL, doi:10.1029/2005GL023234.

Superposed Epoch Analysis of CME/CIR Seed and Radiation Belt Electrons

Storm Time Flux

- Using RBSP map average seed & radiation belt (RB) electron response to CMEs/CIRs vs L^*.
- Figure 5: avg. flux and chorus power for fixed energies vs L^*.
- Figure 6: avg. flux between L^* = 3.5-4, 4-4.5, 4.5-5.
- Epoch t = 0 at min *Dst**, main phase times are normalized to 12 hours.

Figure 5 CME CIR

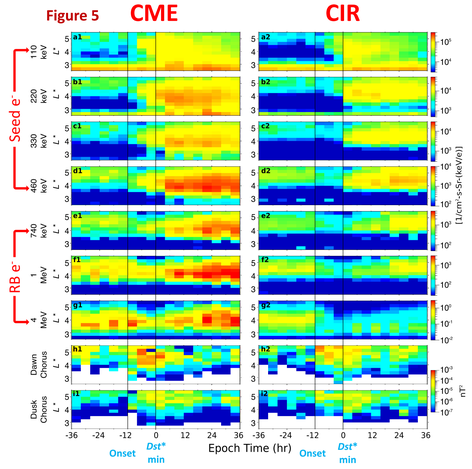

- **Stronger seed enhancement**, which **occurs earlier**, and **penetrates deeper during CME storms** than CIR storms.
- **Stronger radiation belt enhancement in CME storms on average compared to CIR storms.**
- **Earlier seed enhancement provides greater opportunity for local acceleration; more overlap of chorus with strong seed population.**
- **Biggest CME/CIR seed differences are at higher energies/lower L,**
- **Stronger convection** and **more substorm activity gives higher energy electrons more access to lower L** in the inner magnetosphere.

Figure 6

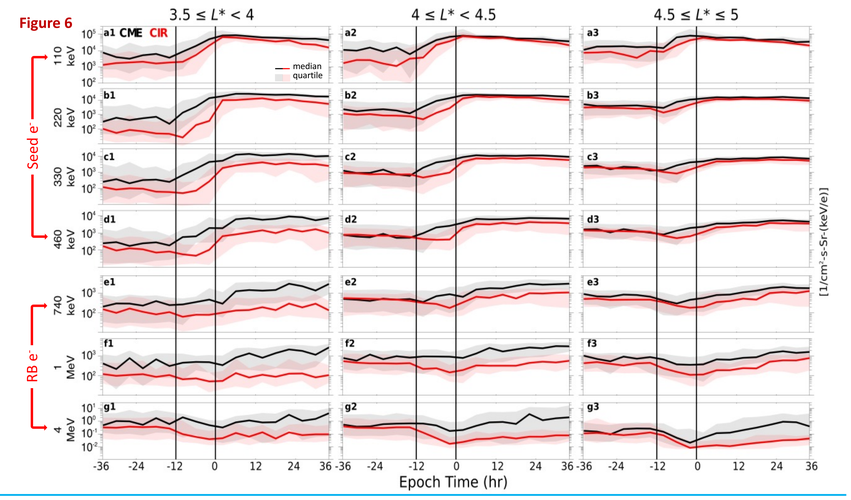

Storm Time Phase Space Density

- Gradients of phase space density (PSD) can reveal aspects of the acceleration, transport, and loss of electron populations.
- Figure 7: avg. MagEIS + Rept PSD vs L^* for fixed μ and K = 0.115 $R_E G^{1/2}$ and chorus wave power.
- Figure 8: Percentage of time an enhancement or loss relative to pre-storm average is observed (> 2*avg, < 0.5*avg).

Figure 7 CME CIR

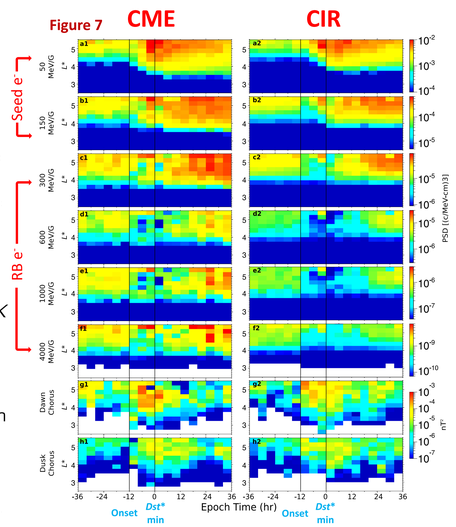

- **Seed population enhancement primarily adiabatic, as PSD is peaked at highest L^*.**
- **CME 150 MeV/G seed population reaches *Boyd et al.* [2015] threshold** of 1×10^{-4} (c/MeV-cm)^3 for acceleration **earlier and more often.**
- **RB enhancement** during **CME** storms occurs **during overlap of chorus activity and seed population well over threshold.**
- **PSD profile of RB CME enhancement has a growing peak around L^* = 4-4.5 for 300-1000 MeV/G electrons – suggests non-adiabatic acceleration.**
- **PSD profile** of **RB during CIR** storms is peaked at highest L*, **RB restoration is adiabatic below L^*=5.5**

Figure 8